GEOPHYSICS, VOL. 62, NO. 1 (JANUARY-FEBRUARY 1997); P. 106–117, 7 FIGS., 1 TABLE.

# Incorporating pore geometry and fluid pressure communication into modeling the elastic behavior of porous rocks

Anthony L. Endres* and Rosemary J. Knight‡

**ABSTRACT**

Inclusion-based formulations allow an explicit description of pore geometry by viewing porous rocks as a solid matrix with embedded inclusions representing individual pores. The assumption commonly used in these formulations that there is no fluid pressure communication between pores is reasonable for liquid-filled rocks measured at high frequencies; however, complete fluid pressure communication should occur throughout the pore space at low frequencies. A generalized framework is presented for incorporating complete fluid pressure communication into inclusion-based formulations, permitting elastic behavior of porous rocks at high and low frequencies to be described in terms of a single model. This study extends previous work by describing the pore space in terms of a continuous distribution of shapes and allowing different forms of inclusion interactions to be specified.

The effects of fluid pressure communication on the elastic moduli of porous media are explored by using simple models and are found to consist of two fundamental elements. One is associated with the cubical dilatation and governs the effective bulk modulus. Its magnitude is a function of the range of pore shapes present. The other is due to the extensional part of the deviatoric strain components and affects the effective shear modulus. This element is dependent on pore orientation, as well as pore shape. Using sandstone and granite models, an inclusion-based formulation shows that large differences between high- and low-frequency elastic moduli can occur for porous rocks. An analysis of experimental elastic wave velocity data reveals behavior similar to that predicted by the models.

Quantities analogous to the open and closed system moduli of Gassmann-Biot poroelastic theory are defined in terms of inclusion-based formulations that incorporate complete fluid pressure communication. It was found that the poroelastic relationships between the open and closed system moduli are replicated by a large class of inclusion-based formulations. This connection permits explicit incorporation of pore geometry information into the otherwise empirically determined macroscopic parameters of the Gassmann-Biot poroelastic theory.

## INTRODUCTION

The elastic properties of porous rocks are dependent on their pore structure and the contained fluids. At seismic frequencies (i.e., less than 2 kHz), the Gassmann-Biot poroelastic theory (Gassmann, 1951; Biot, 1956a,b) satisfactorily describes the elastic wave velocities in porous rocks (Murphy, 1984a). However, this approach cannot be used to predict the dependence of elastic behavior on pore structure because pore geometry information is incorporated through the use of empirically determined macroscopic parameters. A second limitation of this approach is that it cannot be readily extended to consider the elastic behavior of liquid-filled media at high frequencies. The poroelastic assumption of complete fluid pressure communication throughout the pore space becomes invalid as measurement frequency increases (Cleary, 1978). As a result, the Biot formulation underestimates the velocity dispersion commonly observed in porous rocks (Winkler, 1985; Wang and Nur, 1990).

In contrast, inclusion-based models (e.g., Kuster and Toksöz, 1974) incorporate the effects of pore geometry by viewing porous rocks as a solid matrix with embedded inclusions representing the pores. This type of model commonly assumes that

Manuscript received by the Editor February 13, 1995; revised manuscript received June 26, 1996.
*Formerly Waterloo Centre for Groundwater Research, Department of Earth Sciences, University of Waterloo, Waterloo, Ontario N2L 3G1, Canada; presently Boston College, PL/GPE, 29 Randolph Road, Hanscom AFB, MA 01731-3010.
‡Rock Physics Research Program, Department of Geophysics and Astronomy, Department of Geological Sciences, University of British Columbia, Vancouver, British Columbia V6T 1Z4, Canada.
© 1997 Society of Exploration Geophysicists. All rights reserved.

the inclusions are isolated, simulating the conditions encountered in measurements at ultrasonic frequencies (i.e., greater than 100 kHz). Hence, inclusion-based models have been found to be more accurate than the poroelastic theory in describing ultrasonic data (Coyner, 1984; Murphy, 1984a; Wang et al., 1991). However, this approach cannot be used to predict low-frequency behavior.

To permit the direct comparison of laboratory measurements performed at ultrasonic frequencies with surface and borehole data obtained at much lower frequencies, it is necessary to develop a formulation that is valid for both cases. Mavko and Jizba (1991) and Dvorkin and Nur (1993) have attempted to extend the poroelastic theory to the higher frequency regime. However, these formulations continue to use parameters that implicitly incorporate the effects of pore geometry; hence, the problem of quantitatively predicting the effects of pore geometry still exists. The alternate approach is to adapt inclusion-based formulations to the low-frequency range by incorporating interpore fluid pressure communication.

In this paper we expand upon previous results (O'Connell and Budiansky, 1977; Budiansky and O'Connell, 1980) to obtain generalized expressions for effective elastic moduli when interpore fluid pressure communication is incorporated into inclusion-based formulations. The extensions of the previous work presented here are two-fold. First, the pore structure is described as a continuous spectrum of pore shapes instead of a segregation of the pore space into two categories: spherical pores and very thin cracks. Second, different forms of inclusion interaction can be specified; hence, the various inclusion-based formulations that have appeared in the literature can be derived. Using expressions for specific inclusion-based approximations, an equivalence between inclusion-based formulations and the Gassmann-Biot poroelastic theory can be shown. This permits the explicit incorporation of pore geometry information into the definition of poroelastic parameters.

The effects of fluid pressure communication on the elastic properties of porous media are assessed by considering models with various pore shape distributions. The role of interpore fluid pressure communication in the frequency dependent elastic behavior of porous rocks is examined by using the inclusion-based models for three rocks given by Cheng (1978). Experimental data analyzed in this paper exhibit behavior similar to that predicted by these three rock models. The incorporation of fluid pressure communication into inclusion-based models provides insights into the nature of the changes in the elastic behavior of porous rocks that occur over the range of frequencies used in geophysical investigations.

## VOLUMETRIC AVERAGING APPROACH

Two different methods, the volumetric averaging and interaction energy approaches, are used commonly in conjunction with inclusion-based models to determine the effective elastic moduli of a heterogeneous system. First, we will use the volumetric averaging approach (Hill, 1963) to determine the elastic behavior of the porous rock model. The solid matrix has bulk and shear moduli $k_m$ and $\mu_m$, respectively. The pore space is filled with a fluid having a bulk modulus $k_f$; the fluid shear modulus $\mu_f$ is zero. The microscopic structure of the porous rock is uniformly distributed such that its macroscopic elastic response can be equated with an effective homogeneous, isotropic medium with bulk and shear moduli $k^*$ and $\mu^*$, respectively. A representative volume element (RVE) of the porous rock system that is large in comparison to the scale of the inclusions, yet small in contrast to the size of the total system, is selected; the volume of the RVE is $V$. Using the volumetric averaging approach, it can be shown that the cubical dilatation and deviatoric components of the incremental strain tensor, $\partial\theta$ and $\partial e_{ij}$, respectively, in the RVE can be expressed as

$$k^*\langle\partial\theta\rangle_V = k_m\langle\partial\theta\rangle_V + \phi(k_f - k_m)\langle\partial\theta\rangle_{\bar{V}} \tag{1}$$

and

$$\mu^*\langle\partial e_{ij}\rangle_V = \mu_m[\langle\partial e_{ij}\rangle_V - \phi\langle\partial e_{ij}\rangle_{\bar{V}}], \tag{2}$$

where $\langle\cdots\rangle_{V'}$ denotes the volumetric average over a volume $V'$ as given by

$$\langle f\rangle_{V'} = (1/V')\int_{V'} f(\mathbf{x})\,dv, \tag{3}$$

$\bar{V}$ is the volume occupied by the pore space in the RVE, and $\phi = \bar{V}/V$ is the porosity.

Obtaining $k^*$ and $\mu^*$ from equations (1) and (2) requires the determination of the incremental strain within the inclusions representing the individual pores. This is very difficult for an arbitrary pore geometry; however, estimates can be obtained by restricting the inclusions used in the model to specific shapes. For porous rocks, the shape of individual pores can be approximated by oblate spheroidal inclusions. The shape of a pore is characterized by its aspect ratio

$$\alpha = a/b, \tag{4}$$

where $a$ and $b$ are the lengths of the minor and major axes of the inclusion, respectively. The macroscopic isotropy of the system implies that the individual inclusions are randomly oriented. The pore structure in the RVE is described in terms of a volumetric pore shape distribution $\bar{v}(\alpha)$ where

$$\bar{V} = \int_0^1 \bar{v}(\alpha)\,d\alpha. \tag{5}$$

To estimate the incremental strain within the individual pores, an inclusion embedded in a homogeneous, infinite background material having elastic moduli $k_b$ and $\mu_b$ is considered. This system is subjected to an applied incremental strain field that has uniform cubical dilatation and deviatoric components $\partial\theta^A$ and $\partial e_{ij}^A$, respectively, at infinity. The background material and applied incremental strain field used in this analysis are specified such that the interactions between inclusions within the RVE are simulated. From Eshelby (1957), it can be shown that the expected value of the cubical dilatation and deviatoric components of the incremental strain inside a randomly oriented inclusion are (Berryman, 1980b)

$$\partial\theta^{\text{inc}}(\alpha) = P(k_b, \mu_b, k_{\text{inc}}, \mu_{\text{inc}}, \alpha)\partial\theta^A \tag{6}$$

and

$$\partial e_{ij}^{\text{inc}}(\alpha) = Q(k_b, \mu_b, k_{\text{inc}}, \mu_{\text{inc}}, \alpha)\partial e_{ij}^A, \tag{7}$$

respectively, where $k_{\text{inc}}$ and $\mu_{\text{inc}}$ are the bulk and shear moduli of the inclusion material. The terms $P$ and $Q$ are complicated functions defined in Berryman (1980b).

Equations (6) and (7) were derived under the condition that there is no fluid pressure communication between pores. Assuming that all inclusions in the RVE are subjected to the same apparent background material and applied incremental strain fields, the effective elastic moduli obtained from equations (1) and (2) for the case of isolated pores are

$$k^*_{\text{iso}}\langle\partial\theta\rangle_V = k_m\langle\partial\theta\rangle_V + \phi(k_f - k_m)\bar{\gamma}(k_b, \mu_b, k_f, 0)\partial\theta^A \tag{8}$$

and

$$\mu^*_{\text{iso}}\langle\partial e_{ij}\rangle_V = \mu_m\big[\langle\partial e_{ij}\rangle_V - \phi\bar{\chi}(k_b, \mu_b, k_f, 0)\partial e^A_{ij}\big], \tag{9}$$

where

$$\bar{\gamma}(k_b, \mu_b, k_f, 0) = \int_0^1 \bar{c}(\alpha)P(k_b, \mu_b, k_f, 0, \alpha)\,d\alpha, \tag{10}$$

$$\bar{\chi}(k_b, \mu_b, k_f, 0) = \int_0^1 \bar{c}(\alpha)Q(k_b, \mu_b, k_f, 0, \alpha)\,d\alpha \tag{11}$$

and

$$\bar{c}(\alpha) = \bar{v}(\alpha)/\bar{V}. \tag{12}$$

The pore shape spectrum $\bar{c}(\alpha)$ is the probabilistic density function that describes the pore shape distribution per unit volume of porosity.

In the case of complete fluid pressure communication between pores, an incremental fluid pressure change $\partial p_f$ is induced in each pore when the system in the RVE is subjected to an applied incremental strain. Using the Eshelby (1957) approach (see Appendix A), it can be shown that the expected values of the incremental strain components within an individual pore with aspect ratio $\alpha$ under these conditions are

$$\big[\partial\theta^{\text{inc}}(\alpha) + \partial p_f/k_b\big] = \big(\partial\theta^A + \partial p_f/k_b\big)P(k_b, \mu_b, 0, 0, \alpha) \tag{13}$$

and

$$\partial e^{\text{inc}}_{ij}(\alpha) = Q(k_b, \mu_b, 0, 0, \alpha)\partial e^A_{ij}. \tag{14}$$

The incremental change in total pore volume $\partial\bar{V}$ is related to the incremental cubical dilatation within the individual pores and $\partial p_f$ by

$$\partial\bar{V} = \int_0^1 \bar{v}(\alpha)\partial\theta^{\text{inc}}(\alpha)\,d\alpha \tag{15}$$

and

$$\partial p_f = -k_f\partial\bar{V}/\bar{V}, \tag{16}$$

respectively. It follows that the incremental cubical dilatation within an inclusion with aspect ratio $\alpha$ is given by

$$\partial\theta^{\text{inc}}(\alpha) = \frac{(k_b - k_f)P(k_b, \mu_b, 0, 0, \alpha) + k_f\bar{\gamma}(k_b, \mu_b, 0, 0)}{k_f[\bar{\gamma}(k_b, \mu_b, 0, 0) - 1] + k_b}\partial\theta^A. \tag{17}$$

Once again assuming that all inclusions in the RVE are subjected to the same apparent background material and applied incremental strain fields, equations (1) and (2) give the following expressions for the effective elastic moduli when complete fluid pressure communication occurs:

$$k^*_{\text{com}}\langle\partial\theta\rangle_V = k_m\langle\partial\theta\rangle_V + \frac{\phi k_b(k_f - k_m)\bar{\gamma}(k_b, \mu_b, 0, 0)}{k_b + k_f[\bar{\gamma}(k_b, \mu_b, 0, 0) - 1]}\partial\theta^A \tag{18}$$

and

$$\mu^*_{\text{com}}\langle\partial e_{ij}\rangle_V = \mu_m\big[\langle\partial e_{ij}\rangle_V - \phi\bar{\chi}(k_b, \mu_b, 0, 0)\partial e^A_{ij}\big]. \tag{19}$$

The above results are the generalized expressions for the effective elastic moduli that result from the volumetric averaging approach: equations (8) and (9) for the case of isolated pores and equations (18) and (19) when complete pressure communication occurs. To obtain explicit estimates of these moduli, it is necessary to define the nature of the inclusion interactions in the RVE. This will now be done for three specific inclusion-based approximations: the dilute volumetric average, the Kuster-Toksöz and the equivalent inclusion-average stress approximations. In all three cases, it is assumed that the actual solid matrix of the porous rock is equivalent to the apparent background material (i.e., $k_b = k_m$ and $\mu_b = \mu_m$); the inclusion interactions are characterized in terms of the applied incremental strain.

The dilute volumetric average approximation assumes that the inclusion concentration is sufficiently small that interactions between inclusions can be neglected. This implies that the applied incremental strain is identical to the volume average of the incremental strain in the RVE [i.e., $\partial\theta^A = \langle\partial\theta\rangle_V$ and $\partial e^A_{ij} = \langle\partial e_{ij}\rangle_V$]. The following expressions are derived for the dilute volumetric average approximation effective moduli:

$$k^*_{\text{iso}} = k_m + \phi(k_f - k_m)\bar{\gamma}(k_m, \mu_m, k_f, 0), \tag{20}$$

$$\mu^*_{\text{iso}} = \mu_m[1 - \phi\bar{\chi}(k_m, \mu_m, k_f, 0)], \tag{21}$$

$$k^*_{\text{com}} = k_m + \frac{\phi k_m(k_f - k_m)\bar{\gamma}(k_m, \mu_m, 0, 0)}{k_m + k_f[\bar{\gamma}(k_m, \mu_m, 0, 0) - 1]}, \tag{22}$$

and

$$\mu^*_{\text{com}} = \mu_m[1 - \phi\bar{\chi}(k_m, \mu_m, 0, 0)]. \tag{23}$$

Kuster and Toksöz (1974) attempted to overcome dilute inclusion concentration limitations by using a method referred to as the average $T$ matrix approximation (Berryman, 1992). In this approach, a spherical volume of the porous rock system is embedded in an infinite background having moduli $k_m$ and $\mu_m$ and subjected to an applied incremental strain that is uniform at infinity. Its behavior is compared with the response of an identical size homogeneous sphere composed of the effective medium under the same conditions. It is assumed that the elastic wave scattering observed in the far-field is the same for both systems. For the quasi-static case, this condition implies that the volume averages of the incremental stress and strain in the porous medium sphere are equal to the uniform incremental stress and strain in the homogeneous sphere. This

requirement leads to the following relationships between the applied and volumetric average incremental strains:

$$\partial\theta^A = \big(3k^* + 4\mu_m\big)\langle\partial\theta\rangle_V/(3k_m + 4\mu_m), \tag{24}$$

and

$$\partial e_{ij}^A = \big[6\mu^*(k_m + 2\mu_m) + \mu_m(9k_m + 8\mu_m)\big] \times \langle\partial e_{ij}\rangle_V/[5\mu_m(3k_m + 4\mu_m)]. \tag{25}$$

Using these expressions for inclusion interactions, the effective moduli for the Kuster-Toksöz approximation are

$$k_{\text{iso}}^* = \frac{k_m(3k_m + 4\mu_m) + 4\phi\mu_m(k_f - k_m)\bar{\gamma}(k_m, \mu_m, k_f, 0)}{3k_m + 4\mu_m - 3\phi(k_f - k_m)\bar{\gamma}(k_m, \mu_m, k_f, 0)}, \tag{26}$$

$$\mu_{\text{iso}}^* = \mu_m\frac{15k_m + 20\mu_m - \phi(9k_m + 8\mu_m)\bar{\chi}(k_m, \mu_m, k_f, 0)}{15k_m + 20\mu_m + 6\phi(k_m + 2\mu_m)\bar{\chi}(k_m, \mu_m, k_f, 0)}, \tag{27}$$

$$k_{\text{com}}^* = k_m\frac{(3k_m + 4\mu_m)(k_m - k_f) + [k_f(3k_m + 4\mu_m) + 4\phi\mu_m(k_f - k_m)]\bar{\gamma}(k_m, \mu_m, 0, 0)}{(3k_m + 4\mu_m)(k_m - k_f) + [k_f(3k_m + 4\mu_m) - 3\phi k_m(k_f - k_m)]\bar{\gamma}(k_m, \mu_m, 0, 0)}, \tag{28}$$

and

$$\mu_{\text{com}}^* = \mu_m\frac{15k_m + 20\mu_m - \phi(9k_m + 8\mu_m)\bar{\chi}(k_m, \mu_m, 0, 0)}{15k_m + 20\mu_m + 6\phi(k_m + 2\mu_m)\bar{\chi}(k_m, \mu_m, 0, 0)}. \tag{29}$$

However, the Kuster-Toksöz approximation also has concentration limitations; it violates the Hashin-Shtrikman bounds (Hashin and Shtrikman, 1963) when nonspherical inclusions are present in a sufficient quantity (Berryman, 1980a, b).

The third treatment of inclusion interactions that we consider is the equivalent inclusion-average stress (EIAS) approximation (Benveniste, 1987). This approach is consistent with the Hashin-Shtrikman bounds when applied to two-phase systems regardless of the pore shape spectrum (Norris, 1989). The EIAS approach assumes that the applied incremental strain is equal to the volumetric average of the incremental strain in the solid matrix:

$$\langle\partial\theta\rangle_V = (1 - \phi)\partial\theta^A + \phi\langle\partial\theta\rangle_{\bar{V}}, \tag{30}$$

and

$$\langle\partial e_{ij}\rangle_V = (1 - \phi)\partial e_{ij}^A + \phi\langle\partial e_{ij}\rangle_{\bar{V}}. \tag{31}$$

The resulting expressions for the effective elastic moduli of the EIAS formulation are

$$k_{\text{iso}}^* = k_m + \phi(k_f - k_m)\bar{\gamma}(k_m, \mu_m, k_f, 0)\big/\big\{(1 - \phi) + \phi\bar{\gamma}(k_m, \mu_m, k_f, 0)\big\}, \tag{32}$$

$$\mu_{\text{iso}}^* = \mu_m\big\{1 - \phi\bar{\chi}(k_m, \mu_m, k_f, 0)\big/[(1 - \phi) + \phi\bar{\chi}(k_m, \mu_m, k_f, 0)]\big\}, \tag{33}$$

$$k_{\text{com}}^* = k_m + \frac{\phi k_m(k_f - k_m)\bar{\gamma}(k_m, \mu_m, 0, 0)}{(1 - \phi)(k_m - k_f) + [k_f + \phi(k_m - k_f)]\bar{\gamma}(k_m, \mu_m, 0, 0)}, \tag{34}$$

and

$$\mu_{\text{com}}^* = \mu_m\big\{1 - \phi\bar{\chi}(k_m, \mu_m, 0, 0)\big/ [(1 - \phi) + \phi\bar{\chi}(k_m, \mu_m, 0, 0)]\big\}. \tag{35}$$

Other inclusion-based approximations found in the literature that are based on the volumetric averaging principle are obtained by using different descriptions of the inclusion interactions or by varying the averaging procedure. However, it will be seen that these three approximations possess desirable qualities when compared with these other inclusion-based approximations.

## INTERACTION ENERGY APPROACH

In addition to the volumetric averaging method, the interaction energy approach (Eshelby, 1957) has been used to determine the effective elastic moduli from inclusion-based models. This description considers the change in the strain energy within the RVE due to the presence of the inclusions as defined by the relationship

$$E^* = E_m - \Delta E, \tag{36}$$

where $E^*$ is the strain energy in the effective medium, $E_m$ is the strain energy in the matrix material prior to inclusion embedding, and $\Delta E$ is the change in strain energy due to the presence of the inclusions. Surface tractions are applied such that the incremental stress in the RVE is uniform with hydrostatic pressure and deviatoric components $\partial\dot{p}$ and $\partial\dot{s}_{ij}$, respectively. Assuming that the surface tractions are held constant, then

$$E^* = (V/2)\big[\partial\dot{p}^2/k^* + \partial\dot{s}_{ij}\,\partial\dot{s}_{ij}/(2\mu^*)\big] \tag{37}$$

and

$$E_m = (V/2)\big[\partial\dot{p}^2/k_m + \partial\dot{s}_{ij}\,\partial\dot{s}_{ij}/(2\mu_m)\big]. \tag{38}$$

To estimate $\Delta E$, the case of an individual inclusion embedded in a homogeneous, infinite background material is again analyzed. However, this system is now subjected to an applied incremental stress field having uniform hydrostatic pressure and deviatoric components $\partial p^A$ and $\partial s_{ij}^A$, respectively, at infinity. Eshelby (1957) showed that the change in strain energy $\Delta E'$ within this system is given by

$$\Delta E' = (-V_{\text{inc}}/2)\big(-\partial\theta^T\,\partial p^A + \partial e_{ij}^T\,\partial s_{ij}^A\big), \tag{39}$$

where $V_{\text{inc}}$ is the volume of the inclusion and $\partial\theta^T$ and $\partial e_{ij}^T$ are the cubical dilatation and deviatoric components, respectively, of the incremental "stress-free transformation" strain. From

the Eshelby (1957) equivalent inclusion analysis, it can be shown that the expected values of the incremental "stress-free transformation" strain components for a randomly oriented isolated inclusion with aspect ratio $\alpha$ are given by

$$\partial\theta^T(\alpha) = (k_f - k_b)P(k_b, \mu_b, k_f, 0, \alpha)\partial p^A / k_b^2 \quad (40)$$

and

$$\partial e_{ij}^T(\alpha) = Q(k_b, \mu_b, k_f, 0, \alpha)\partial s_{ij}^A / (2\mu_b). \quad (41)$$

From Appendix A and equations (15)–(17), it can be shown that the expected values of the incremental "stress-free transformation" strain components for an identically shaped inclusion when complete pressure communication occurs are

$$\partial\theta^T(\alpha) = (k_b - k_f)P(k_b, \mu_b, 0, 0, \alpha)\partial p^A / \left\{k_b\left\{k_f[1 - \bar{\gamma}(k_b, \mu_b, 0, 0)] - k_b\right\}\right\} \quad (42)$$

and

$$\partial e_{ij}^T(\alpha) = Q(k_b, \mu_b, 0, 0, \alpha)\partial s_{ij}^A / (2\mu_b). \quad (43)$$

Using these results, the following generalized expressions are derived for the effective elastic moduli of the porous medium. In the case where all inclusions are totally isolated,

$$\partial \dot{p}^2 / k_{\text{iso}}^* = \partial \dot{p}^2 / k_m + \phi(k_b - k_f) \times \bar{\gamma}(k_b, \mu_b, k_f, 0)(\partial p^A)^2 / (k_b^2) \quad (44)$$

and

$$\partial \dot{s}_{ij}\, \partial \dot{s}_{ij} / \mu_{\text{iso}}^* = \partial \dot{s}_{ij}\, \partial \dot{s}_{ij} / \mu_m + \phi\bar{\chi}(k_b, \mu_b, k_f, 0) \times \partial s_{ij}^A\, \partial s_{ij}^A / \mu_b. \quad (45)$$

When complete fluid pressure communication occurs throughout the pore space,

$$\frac{\partial \dot{p}^2}{k_{\text{com}}^*} = \frac{\partial \dot{p}^2}{k_m} + \frac{\varphi(k_f - k_b)\bar{\gamma}(k_b, \mu_b, 0, 0)}{k_b\{k_f[1 - \bar{\gamma}(k_b, \mu_b, 0, 0)] - k_b\}}(\partial p^A)^2 \quad (46)$$

and

$$\partial \dot{s}_{ij}\, \partial \dot{s}_{ij} / \mu_{\text{com}}^* = \partial \dot{s}_{ij}\, \partial \dot{s}_{ij} / \mu_m + \phi\bar{\chi}(k_b, \mu_b, 0, 0) \times \partial s_{ij}^A\, \partial s_{ij}^A / \mu_b. \quad (47)$$

The specific interaction energy approximation of interest uses the dilute inclusion concentration assumption proposed in Eshelby (1957) (i.e., $k_b = k_m, \mu_b = \mu_m, \partial p^A = \partial \dot{p}$ and $\partial s_{ij}^A = \partial \dot{s}_{ij}$). This dilute condition differs from that used in the volumetric averaging approach in that $\partial\theta^A = (k^*/k_m)\partial\dot{\theta}$ and $\partial e_{ij}^A = (\mu^*/\mu_m)\partial \dot{e}_{ij}$. Hence, the dilute interaction energy approximation gives the following expressions for the effective moduli:

$$k_{\text{iso}}^* = k_m^2 / [k_m + \phi(k_m - k_f)\bar{\gamma}(k_m, \mu_m, k_f, 0)], \quad (48)$$

$$\mu_{\text{iso}}^* = \mu_m / [1 + \phi\bar{\chi}(k_m, \mu_m, k_f, 0)], \quad (49)$$

$$k_{\text{com}}^* = k_m \frac{k_f[1 - \bar{\gamma}(k_m, \mu_m, 0, 0)] - k_m}{k_f - k_m + [\phi(k_f - k_m) - k_f]\bar{\gamma}(k_m, \mu_m, 0, 0)}, \quad (50)$$

and

$$\mu_{\text{com}}^* = \mu_m / [1 + \phi\bar{\chi}(k_m, \mu_m, 0, 0)]. \quad (51)$$

The expressions for $k_{\text{com}}^*$ and $\mu_{\text{com}}^*$ obtained from the volumetric averaging [equations (18) and (19)] and interaction energy [equations (46) and (47)] approaches are generalized versions of the results given in Budiansky and O'Connell (1980). Unlike the previous work where the pore space is divided into two shapes (i.e., spheres with $\alpha = 1$ and very thin cracks with $\alpha \approx 0$), the pore geometry is now described in terms of a continuous shape spectrum. In addition, various inclusion-based formulations that have appeared in the literature can now be obtained directly from this new result by defining different descriptions of inclusion interactions in terms of the apparent background moduli and applied incremental strain or stress.

## RELATIONSHIP TO GASSMANN-BIOT THEORY

In the static limit, the Gassmann-Biot theory relates the elastic response of a porous medium under open and closed conditions. An open (i.e., drained) system permits the pore fluid to cross the boundaries of the porous medium freely with changes in the applied conditions. There is no incremental pore fluid pressure change caused by this process. Pore fluid is confined within the system during variations in applied conditions under closed (i.e., undrained) conditions. Gassmann (1951) showed that the bulk moduli under open and closed conditions, $k_{\text{open}}$ and $k_{\text{closed}}$, respectively, are related by

$$k_{\text{closed}} = k_m \frac{k_f(k_m - k_{\text{open}}) + \phi k_{\text{open}}(k_m - k_f)}{k_f(k_m - k_{\text{open}}) + \phi k_m(k_m - k_f)}. \quad (52)$$

Assuming that there is no change in total pore volume because of an applied shear stress, Gassmann argued that the compressibility of the pore fluid does not affect the shear modulus of the overall system; hence,

$$\mu_{\text{closed}} = \mu_{\text{open}}. \quad (53)$$

Using the inclusion-based formulations derived for complete pressure communication, analogs for the open and closed system moduli of the poroelastic theory can be defined. The inclusion-based moduli $k_{\text{com}}^*$ and $\mu_{\text{com}}^*$ are the counterparts of $k_{\text{closed}}$ and $\mu_{\text{closed}}$ in the poroelastic theory. The open-system conditions are replicated in the inclusion-based formulations by using an infinitely compressible fluid (i.e., $k_f = 0$). Using this condition in the expressions for $k_{\text{com}}^*$ and $\mu_{\text{com}}^*$, the inclusion-based equivalents of the open-system moduli $k_{\text{open}}^*$ and $\mu_{\text{open}}^*$ are obtained.

For the dilute volumetric average, Kuster-Toksöz, EIAS and dilute interaction energy approximations, it can be shown that the relationship between the inclusion-based analogs for the open and closed system moduli are identical to the Gassmann (1951) poroelastic relationships. This is accomplished by replacing $k_{\text{open}}$ and $\mu_{\text{open}}$ in equations (52) and (53) with the expressions obtained for $k_{\text{open}}^*$ and $\mu_{\text{open}}^*$ from each of these

approximations. The open-system moduli for these four approximations are given in Appendix B. After some algebraic manipulation, it is found that $k_{\text{closed}} = k^*_{\text{com}}$ and $\mu_{\text{closed}} = \mu^*_{\text{com}}$ for each approximation. An example of this procedure for the dilute volumetric average approximation is shown in Appendix B. Previously, Thomsen (1985) reported a similar result for a dilute concentration version of the Budiansky and O'Connell (1980) formulation.

In addition to these four inclusion-based approximations, formulations using the self-consistency condition to simulate inclusion interactions (Wu, 1966; Budiansky and O'Connell, 1976; Korringa et al., 1979; Berryman, 1980a,b) and the differential effective medium (DEM) approximation (Norris, 1985) have been used to analyze the elastic behavior of porous rocks. When expressions for $k^*_{\text{com}}$ and $\mu^*_{\text{com}}$ for these approximations were derived using the framework presented in this paper, it was found that the connections between the resulting inclusion-based analogs for open and closed system moduli are not described by the Gassmann (1951) poroelastic relationships. The initial work in Budiansky and O'Connell (1980) used a self-consistent formulation; hence, their result is also not consistent with the Gassmann-Biot theory, as earlier reported by Thomsen (1985). While the reason for this is not clear immediately, both the self-consistency assumption and the DEM approximation imply definite hierarchical relationships in the structure of the medium (Milton, 1984).

Thomsen (1985) and Berryman (1992) have proposed methods to overcome violation of the Gassmann (1951) poroelastic relationships by the self-consistent and DEM approximations. Our implementation of the Thomsen (1985) scheme found that the resulting inclusion-based analogs for open and closed system moduli satisfied the Gassmann (1951) relationships when only spherical pores are used. The results given by Berryman (1992) are limited to spherical inclusions due to the complexity of the scattering technique used in the analysis of inclusion response when applied to nonspherical inclusions. Given the special nature of spherical inclusions (which will be illustrated in the modeling section), it is not readily apparent that the Berryman (1992) approach would be successful when nonspherical pores are used.

This equivalence between the Gassmann-Biot theory and the dilute volumetric average, Kuster-Toksöz, EIAS and dilute interaction energy approximations allows definition of poroelastic parameters, which have generally been treated as empirical quantities, in terms of pore space geometry. Further, all four approximations have explicit, closed-form expressions for the effective elastic moduli that permit easy computation. A similar definition of the Gassmann-Biot open-system moduli in terms of an inclusion-based model was suggested by Korringa and Thompson (1977); however, its equivalence could not be demonstrated because of their use of a self-consistent formulation.

## MODELING RESULTS

In this section, the relationship between pore structure and the effects of fluid pressure communication will be examined using inclusion-based models. This is accomplished by considering models for porous media where the pore space geometry is described in terms of discrete pore shape spectra. For a porous medium with $N$ discrete pore shapes, the following quantities in the inclusion-based formulations are given by

$$\bar{\gamma}(k_b, \mu_b, k_f, 0) = \sum_{n=1}^{N} \bar{c}(\alpha_n) P(k_b, \mu_b, k_f, 0, \alpha_n), \quad (54)$$

and

$$\bar{\chi}(k_b, \mu_b, k_f, 0) = \sum_{n=1}^{N} \bar{c}(\alpha_n) Q(k_b, \mu_b, k_f, 0, \alpha_n). \quad (55)$$

Let us consider a series of "sphere-crack" models that have pore shape spectra containing two shapes: spheres ($\alpha_1 = 1$) and identically shaped "cracks" ($\alpha_2 < 1$). These models differ from those used in Budiansky and O'Connell (1980) by permitting the cracks to have nonzero aspect ratios. The pore shape spectrum for a given model is uniquely specified by $\alpha_2$ and the volume fraction of the pore space composed of cracks [i.e., crack fraction $\bar{c}(\alpha_2) = 1 - \bar{c}(\alpha_1)$]. The pore fluid is assumed to be water; hence, $k_f = 2.32$ GPa. The elastic moduli for the rock matrix are $k_m = 30$ GPa and $\mu_m = 17$ GPa. The porosity was maintained constant at $\phi = 0.1$ for all sphere-crack models. Given the favorable inclusion concentration limitations of the EIAS approximation, it was used to determine the effective moduli for the cases of isolated inclusions [equations (32) and (33)] and complete fluid pressure communication [equations (34) and (35)]. The relative differences in $k^*$ [i.e., $\Delta k^*_{\text{rel}} = (k^*_{\text{iso}} - k^*_{\text{com}})/k^*_{\text{com}}$] and $\mu^*$ [i.e., $\Delta\mu^*_{\text{rel}} = (\mu^*_{\text{iso}} - \mu^*_{\text{com}})/\mu^*_{\text{com}}$] as functions of $\bar{c}(\alpha_2)$ for various $\alpha_2$ values are shown in Figures 1 and 2, respectively.

The effects of fluid pressure communication on the elastic moduli of porous media consist of two fundamental elements. One is associated with the cubical dilatation and governs $k^*$. The other is caused by the extensional part of the deviatoric strain components and affects $\mu^*$. The magnitude of the volume change for a pore caused by a given $\partial\theta^A$ increases as its aspect ratio decreases. Because $\partial\theta^A$ is a scalar quantity, this volume change is independent of the pore orientation. Hence, the incremental fluid pressure change is the same in identically shaped pores. When only a single pore shape is present, the

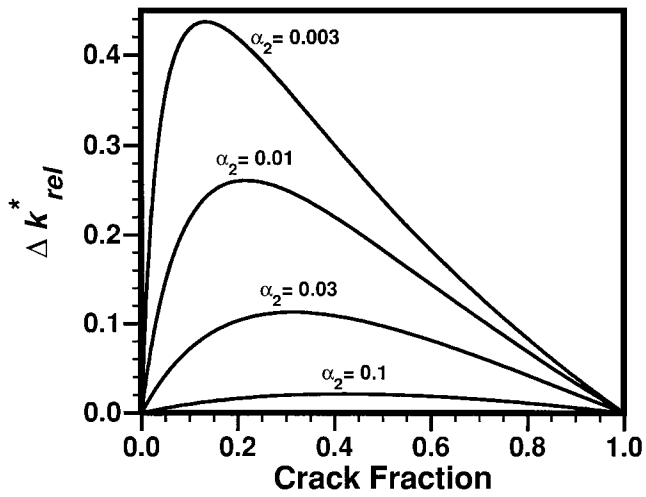


FIG. 1. Relative difference in $k^*$ [i.e., $\Delta k^*_{\text{rel}} = (k^*_{\text{iso}} - k^*_{\text{com}})/k^*_{\text{com}}$] for water-filled sphere-crack models as a function of crack fraction [$\bar{c}(\alpha_2)$]. Crack aspect ratio ($\alpha_2$) for models are denoted on the figure.

incremental fluid pressure is the same throughout the entire pore space whether pores are isolated or complete pressure communication occurs. This leads to the result $k^*_{iso} = k^*_{com}$ in this circumstance. This is seen in Figure 1 where $\Delta k^*_{rel}$ goes to zero when $\bar{c}(\alpha_2)$ equals 0 or 1.

When both spheres and cracks are present [i.e., $0 < \bar{c}(\alpha_2) < 1$], the effects of fluid pressure communication conditions on $k^*$ become apparent. The induced fluid pressure change in the cracks is greater than in the spheres. When there is fluid pressure communication between the pores, excess fluid pressure in the cracks is relieved by fluid moving to the lower pressure regime in the spheres. Effectively, the communicating cracks are softened relative to their state when pores are isolated. This implies that $k^*_{iso} > k^*_{com}$ and $\Delta k^*_{rel} > 0$. This effect increases as the crack aspect ratio decreases; this is seen on Figure 1 as increasing values of $\Delta k^*_{rel}$ are obtained as $\alpha_2$ decreases when $\bar{c}(\alpha_2)$ is held constant.

The dependence of $\Delta k^*_{rel}$ on the crack fraction $\bar{c}(\alpha_2)$ is the result of two competing factors, resulting in the maximum in $\Delta k^*_{rel}$ that is observed in Figure 1 for all values of $\alpha_2$. The initial replacement of the spheres by cracks [i.e., as $\bar{c}(\alpha_2)$ increases from 0.0] leads to a more rapid increase in pore space compressibility for the complete pressure communication case than that which occurs when the pores are isolated; this leads to increasing $\Delta k^*_{rel}$ values. However, this replacement of the spheres reduces the volume of lower pressure regime into which the cracks expel their contents. This causes the difference in pore space compressibility between the two pressure conditions to lessen. Eventually, this results in decreasing $\Delta k^*_{rel}$ once some critical value of $\bar{c}(\alpha_2)$ is reached. As $\alpha_2$ decreases, this critical value of $\bar{c}(\alpha_2)$ occurs at lower crack fractions, resulting in a shift of the maximum $\Delta k^*_{rel}$ value.

The extensional part of $\partial e^A_{ij}$ causes a volume change in an individual pore which is dependent on its orientation with respect to $\partial e^A_{ij}$, as well as its shape. In the case of randomly oriented isolated pore spaces, this results in induced fluid pressure variations among pores of the same shape and a coupling between $\partial e^{inc}_{ij}(\alpha)$ and $k_f$ in the nonspherical pores. For spherical pores, $\partial e^A_{ij}$ will always be a purely shear strain (i.e., zero extensional components); hence, there is zero incremental pore volume change and no resultant coupling between $\partial e^{inc}_{ij}(\alpha)$ and $k_f$. When the cumulative volume change of the individual pores is considered, it is found that there is no overall change in the total pore volume. Since it is the total pore volume variation that controls the induced fluid pressure change in the complete pressure communication case, the zero total pore volume change results in a decoupling of $\partial e^{inc}_{ij}(\alpha)$ from $k_f$. This means a communicating pore responds in the same manner as an identically shaped cavity to a given $\partial e^A_{ij}$.

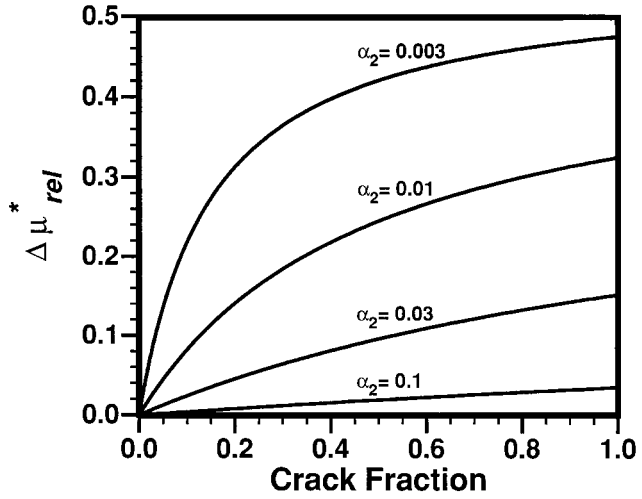


FIG. 2. Relative difference in $\mu^*$ [i.e., $\Delta\mu^*_{rel} = (\mu^*_{iso} - \mu^*_{com})/\mu^*_{com}$] for water-filled sphere-crack models as a function of crack fraction [$\bar{c}(\alpha_2)$]. Crack aspect ratio ($\alpha_2$) for models are denoted on the figure.

This difference in the coupling between $\partial e^{inc}_{ij}(\alpha)$ and $k_f$ for the two pressure communication conditions implies that $\mu^*_{iso} \geq \mu^*_{com}$ and $\Delta\mu^*_{rel} \geq 0$. As $\bar{c}(\alpha_2)$ increases, isolated spheres where no coupling occurs are replaced by isolated cracks in which coupling takes place; hence, $\Delta\mu^*_{rel}$ monotonically increases as shown in Figure 2. This coupling effect is enhanced in Figure 2 as $\alpha_2$ decreases due to the increased coupling that happens in an isolated pore as its aspect ratio shrinks.

If only spherical pores are present, there is no induced fluid pressure within the pores due to $\partial e^A_{ij}$ regardless of the nature of the interpore pressure communication. Thus, the effective shear modulus is independent of $k_f$; and, $\mu^*_{iso} = \mu^*_{com}$. This produces the zero $\Delta\mu^*_{rel}$ value at $\bar{c}(\alpha_2) = 0$ in Figure 2. This condition, combined with the fact that $k^*_{iso} = k^*_{com}$ when a single shape is present, explains the equivalence between the Kuster-Toksöz approximation using isolated spherical inclusions and the Gassmann-Biot formulation noted in Toksöz et al. (1976).

The effects of fluid pressure communication on the elastic moduli of porous rocks were examined by using the Berea sandstone, Boise sandstone, and Troy granite models given in Cheng (1978). The pore shape spectra for these rocks are estimates for the pore geometry at zero effective pressure based on the fitting of velocity-effective pressure data using the Kuster-Toksöz approximation. The pore shape spectra for these models are shown in Figure 3, and rock matrix moduli and porosities are given in Table 1. The effective moduli were determined using the Kuster-Toksöz approximation [equations (26)–(29)], and $\Delta k^*_{rel}$ and $\Delta\mu^*_{rel}$ for $k_f$ values between 100 kPa and 10 GPa are shown in Figures 4 and 5, respectively. A large portion of this range of $k_f$ values can be viewed as the behavior of a partially saturated rock when air (155 kPa) and water (2.32 GPa) are the pore fluids. The response of these models indicates that the variation in the elastic moduli of a porous rock due to changes in fluid pressure communication can be very large. The maximum relative change is greater for $k^*$ (i.e., on the order of one to five times $k^*_{com}$) than for $\mu^*$ (i.e., 20% to 40% of $\mu^*_{com}$). Since the case of isolated inclusions corresponds to conditions at the high-frequency limit and complete pressure communication occurs at the low-frequency limit, large differences are

**Table 1. Matrix elastic moduli and porosity for the Berea sandstone, Boise sandstone and Troy granite models from Cheng (1978).**

| | Berea sandstone | Boise sandstone | Troy granite |
|---|---|---|---|
| $k_m$ (in GPa) | 33.0 | 30.0 | 70.0 |
| $\mu_m$ (in GPa) | 24.5 | 17.0 | 35.0 |
| $\phi$ | 16.3% | 25.0% | 0.33% |

predicted in the elastic moduli determined from ultrasonic and seismic frequency measurements.

The responses of all the rock models have common features. The difference in the induced fluid pressure between the low and high aspect ratio pores grows as $k_f$ initially increases; hence, the effects of fluid pressure relaxation in the lower aspect ratio pores are amplified. This leads to the increasing $\Delta k^*_{\text{rel}}$ observed in Figure 4. However, the amount of pore volume change decreases as $k_f$ approaches the magnitude of the rock matrix moduli; this acts to decrease the effects of fluid pressure relaxation in the crack and decreases $\Delta k^*_{\text{rel}}$. Hence, there is a tradeoff between these competing mechanisms as $k_f$ increases; this results in a maximum value in $\Delta k^*_{\text{rel}}$ and its decrease in Figure 4. The value of $\Delta\mu^*_{\text{rel}}$ increases monotonically with increasing $k_f$ in Figure 5 as the magnitude of the coupling in the isolated nonspherical pores grows and $\mu^*_{\text{com}}$ remains constant.

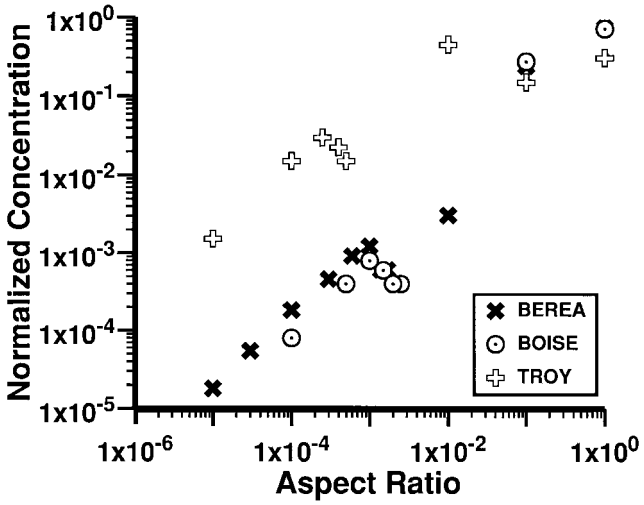


FIG. 3. Pore shape spectrum for Berea sandstone, Boise sandstone, and Troy granite from Cheng (1978).

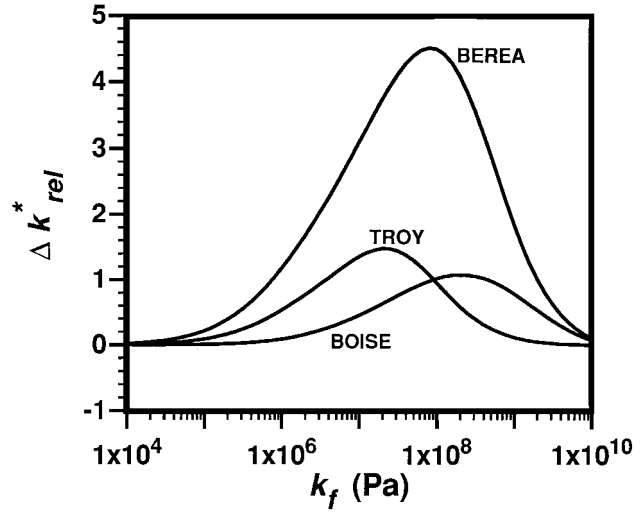


FIG. 4. Relative difference in $k^*$ [i.e., $\Delta k^*_{\text{rel}} = (k^*_{\text{iso}} - k^*_{\text{com}})/k^*_{\text{com}}$] as a function of fluid bulk modulus ($k_f$) for Berea sandstone, Boise sandstone, and Troy granite models.

## EXPERIMENTAL EVIDENCE

The behavior exhibited in Figures 4 and 5 can be observed in published laboratory results. Although the corresponding measurements for the samples analyzed by Cheng (1978) are not available, there are other ultrasonic elastic wave velocity data appropriate for testing the modeling results. Specifically, we will examine velocity data for partially saturated specimens of Cotton Valley sandstone (Murphy, 1984b), Sierra White granite (Murphy, 1984a), Spirit River sandstone (Knight and Nolen-Hoeksema, 1990), and Travis Peak (W-5A) sandstone (Gregory, 1976); the pore fluids in these samples were air and distilled water (2.237 GPa). These rocks were selected for their low permeability and porosity, features that we believe make the assumption of negligible fluid pressure communication between liquid-filled pores at ultrasonic frequencies reasonable. The relative differences in $k$ [i.e., $\Delta k_{\text{rel}} = (k_{\text{high}} - k_{\text{low}})/k_{\text{low}}$] and $\mu$ [i.e., $\Delta\mu_{\text{rel}} = (\mu_{\text{high}} - \mu_{\text{low}})/\mu_{\text{low}}$] were determined for each rock; the subscripts "high" and "low" denote the elastic moduli in the high and low frequency ranges.

The data used for this analysis are measurements of velocity as a function of overall water saturation $S_w$. For comparison with the modeling study, it is necessary to convert these data from $S_w$ into an effective bulk modulus for the pore filling. This condition is satisfied at the low-frequency limit where the contents of the entire pore space in a partially saturated medium behave as a single pore fluid; the effective bulk modulus $k_{\text{eff}}$ of this mixture is

$$k_{\text{eff}} = k_a k_w / [S_w k_a + (1 - S_w) k_w], \tag{56}$$

where $k_a$ and $k_w$ are the bulk moduli of air and water, respectively. The results of this analysis are expressed in terms of $k_{\text{eff}}$ defined by equation (56).

To achieve a corresponding situation at the high-frequency limit, it would be required that the individual pores contain a macroscopically homogeneous mixture of air and water (i.e., small air bubbles in the water phase) that is uniformly distributed throughout the entire pore space. The experimental

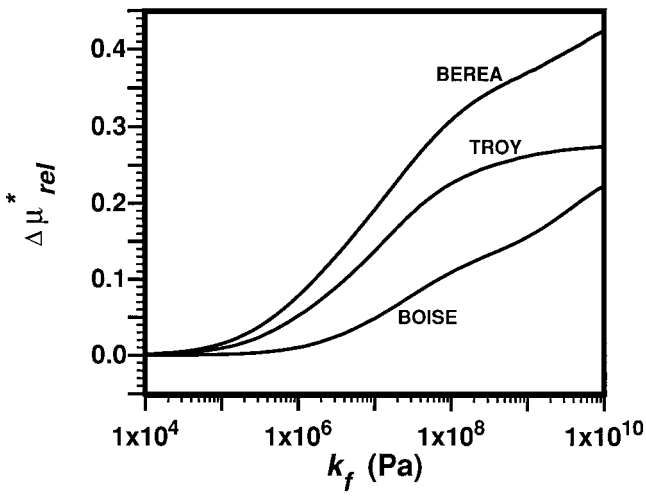


FIG. 5. Relative difference in $\mu^*$ [i.e., $\Delta\mu^*_{\text{rel}} = (\mu^*_{\text{iso}} - \mu^*_{\text{com}})/\mu^*_{\text{com}}$] as a function of fluid bulk modulus ($k_f$) for Berea sandstone, Boise sandstone, and Troy granite models.

data considered here controlled $S_w$ by evaporative drying. This produces a different pore scale fluid distribution where individual pore spaces tend to be either air or water saturated. The pore fluid bulk modulus for an individual pore at the high-frequency limit is either $k_a$ or $k_w$, not the effective bulk modulus $k_{\text{eff}}$. Modeling results suggest that while the details of this analysis will differ for the evaporative drying and macroscopically homogeneous mixture cases when expressed in terms of $k_{\text{eff}}$, the general form and magnitude of $\Delta k_{\text{rel}}$ and $\Delta \mu_{\text{rel}}$ will be similar for these two saturation techniques.

The values of $\Delta k_{\text{rel}}$ and $\Delta \mu_{\text{rel}}$ were computed for these four rock samples using the method given in Winkler (1986). The solid matrix bulk moduli used in this analysis were 56 GPa for the granite and 33 GPa for the sandstones. A suggestion was made by Winkler (1986) to treat the pore space volume occupied by surface bound water as part of an effective rock matrix. In this case, the wetted matrix system is used for estimating the open system moduli, and both the porosity and water saturation values are adjusted to reflect this redefinition of the rock system. This was done for the Spirit River sandstone that shows a pronounced effect caused by the bound water in both the elastic wave velocity and the dielectric properties (Knight and Nur, 1987) at low saturations (i.e., for $S_w < 0.30$ in the case of the velocity data).

The results of this analysis for $\Delta k_{\text{rel}}$ and $\Delta \mu_{\text{rel}}$ are shown in Figures 6 and 7, respectively. The modeling results given in Figures 4 and 5 are also shown for reference. Due to the nonlinear relationship between $k_{\text{eff}}$ and $S_w$, the $S_w$ range from 0.00 to 0.99 covers $k_{\text{eff}}$ values from 155 kPa to 15.4 MPa. Hence, there is a large region of $k_{\text{eff}}$ values between 15.4 MPa and 2.24 GPa, corresponding to $S_w$ values between 0.99 and 1.00, that cannot be resolved by the data.

Overall, it can be seen that the general features predicted in Figures 4 and 5 are reproduced by the experimental data shown in Figures 6 and 7, respectively. The quantity $\Delta k_{\text{rel}}$ in Figure 6 grows substantially as $k_{\text{eff}}$ increases, obtaining a magnitude for its maximum value comparable to that shown in Figure 4 (i.e., on the order of one to five). Further, it can be seen that the $\Delta k_{\text{rel}}$ values at $S_w = 1.00$ are significantly below its maximum for the three cases where measurements at full saturation were taken (i.e., Cotton Valley, Sierra White, and Travis Peak). This establishes the presence of the relative maximum exhibited in Figure 4. Figure 7 shows an increasing $\Delta \mu_{\text{rel}}$ as $k_{\text{eff}}$ increases, with the maximum values between 0.1 and 0.5, simulating the behavior on Figure 5. As predicted, the effects of changing $k_{\text{eff}}$ are greater for $\Delta k_{\text{rel}}$ than for $\Delta \mu_{\text{rel}}$.

## CONCLUSIONS

A general framework for incorporating fluid pressure communication into inclusion-based models for porous rocks has been presented. This allows the use of inclusion-based formulations to model the elastic response of porous rocks over a wide range of measurement frequencies. Two significant results are the proven equivalence of a large class of inclusion-based approximations with the Biot-Gassmann poroelastic theory and the illustrated dependence of the elastic moduli on fluid pressure communication and pore geometry.

Our inclusion-based formulation allows for the use of different forms of inclusion interactions. In particular, expressions corresponding to the dilute volumetric average, Kuster-Toksöz, EIAS and dilute interaction energy approximations were derived. All four of these approximations were found to replicate the Gassmann (1951) relationships. The equivalence between these inclusion-based approximations and the poroelastic theory permits the explicit use of pore geometry information in determining poroelastic parameters that must otherwise be empirically obtained. Further, this link allows poroelastic

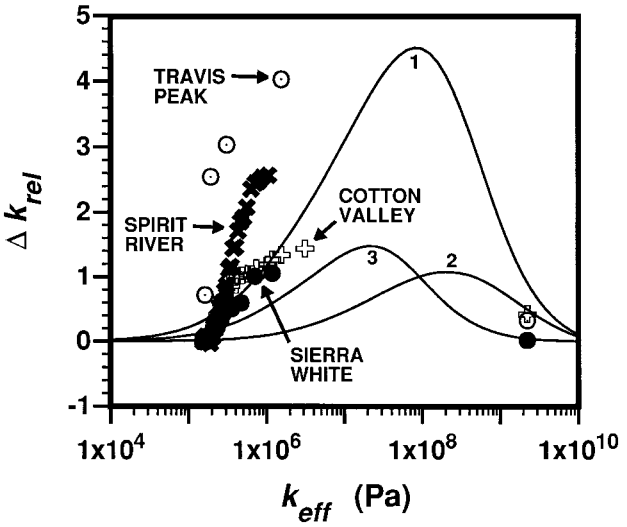


FIG. 6. Relative difference in $k$ [i.e., $\Delta k_{\text{rel}} = (k_{\text{high}} - k_{\text{low}})/k_{\text{low}}$] as a function of effective fluid bulk modulus ($k_{\text{eff}}$) determined from ultrasonic elastic wave velocity data for partially saturated specimens of Cotton Valley sandstone-✣, Sierra White granite-●, Spirit River sandstone-✖ and Travis Peak sandstone-⊙. The modeling results for Berea sandstone-1, Boise sandstone-2, and Troy granite-3 from Figure 4 are shown for reference.

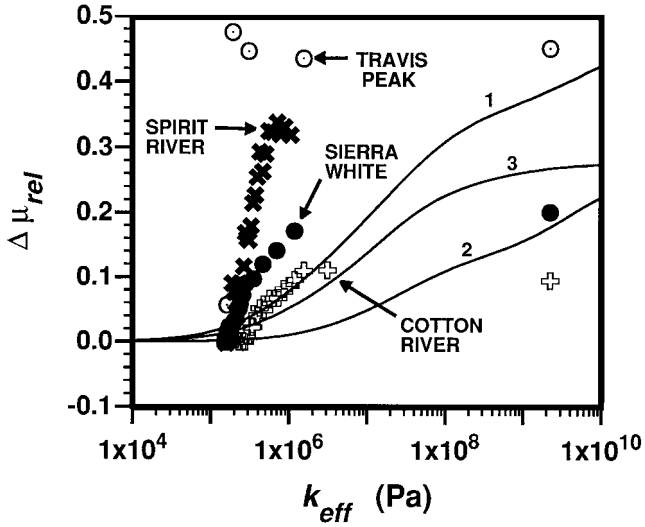


FIG. 7. Relative difference in $\mu$ [i.e., $\Delta \mu_{\text{rel}} = (\mu_{\text{high}} - \mu_{\text{low}})/\mu_{\text{low}}$] as a function of effective fluid bulk modulus ($k_{\text{eff}}$) determined from ultrasonic elastic wave velocity data for partially saturated specimens of Cotton Valley sandstone-✣, Sierra White granite-●, Spirit River sandstone-✖, and Travis Peak sandstone-⊙. The modeling results for Berea sandstone-1, Boise sandstone-2, and Troy granite-3 from Figure 5 are shown for reference.

behavior to be related to other physical properties that can be described in terms of inclusion-based formulations, such as dielectric permittivity (Endres and Knight, 1991).

The effects of fluid pressure communication and its relationship to pore space geometry were investigated by determining the effective elastic moduli for models with various pore shape spectra. The effects of the fluid pressure communication on the elastic moduli of porous rocks consist of two fundamental elements. One is associated with the extensional part of the deviatoric strain components and controls the effective shear modulus. The other is caused by the cubical dilatation and governs the effective bulk modulus. The former is dependent on the pore shape and orientation; the latter is a function of only pore shape.

Using models given in Cheng (1978) for two sandstones and a granite, it was found that the variation in the elastic moduli of a porous rock due to changes in fluid pressure communication conditions can be very large. An analysis of experimental data for three sandstones and a granite revealed similar effects in the observed behavior of porous rocks. Since the cases of isolated inclusions and complete pressure communication correspond to the conditions at the high- and low-frequency limits, respectively, large differences are predicted in the elastic moduli determined from ultrasonic and seismic frequency measurements. This leads to elastic wave velocity dispersion due to the local flow or fluid squirt mechanism (Jones, 1986; Murphy et al., 1986). While other factors, such as inertial and scattering phenomena, affect elastic wave propagation, the results of this paper indicate that the changes in fluid pressure communication can result in large changes in the effective elastic moduli of a porous rock which would produce significant elastic wave velocity dispersion.

## ACKNOWLEDGMENTS

A. L. Endres was supported by a postdoctoral fellowship from the Natural Sciences and Engineering Research Council (NSERC) of Canada and funding from the Waterloo Centre for Groundwater Research during this work. Financial support for research by R. J. Knight was obtained through an NSERC IOR grant with funding from Imperial Oil, Petro-Canada, and Shell Canada.

## REFERENCES

Benveniste, Y., 1987, A new approach to the application of Mori-Tanaka's theory in composite materials: Mech. Mater., **6**, 147–157.

Berryman, J. G., 1980a, Long-wavelength propagation in composite elastic media I. Spherical inclusions: J. Acoust. Soc. Am., **68**, 1809–1819.

——— 1980b, Long-wavelength propagation in composite elastic media II. Ellipsoidal inclusions: J. Acoust. Soc. Am., **68**, 1820–1831.

——— 1992, Single-scattering approximations for coefficients in Biot's equations of poroelasticity: J. Acoust. Soc. Am., **91**, 551–571.

Biot, M. A., 1956a, Theory of propagation of elastic waves in fluid-saturated porous solids. I. low-frequency range: J. Acoust. Soc. Am., **28**, 168–178.

——— 1956b, Theory of propagation of elastic waves in fluid-saturated porous solids. II. higher frequency range: J. Acoust. Soc. Am., **28**, 179–191.

Budiansky, B., and O'Connell, R. J., 1976, Elastic moduli of a cracked solid: Int. J. Solids Structures, **12**, 81–97.

——— 1980, Bulk dissipation in heterogeneous media, *in* Nemat-Nasser, S., Ed., Solid earth geophysics and geotechnology: Am. Soc. Mech. Eng., 1–10.

Cheng, C. H., 1978, Seismic velocities in rock: Direct and inverse problems: Sc.D. thesis, Massachusetts Inst. Tech.

Cleary, M. P., 1978, Elastic and dynamic response regimes of fluid-impregnated solids with diverse microstructures: Int. J. Solids Structures, **14**, 795–819.

Coyner, K. B., 1984, Effects of stress, pore pressure, and pore fluids on bulk strain, velocity, and permeability in rocks: Ph.D. thesis, Massachusetts Inst. Tech.

Dvorkin, J., and Nur, A., 1993, Dynamic poroelasticity: A unified model with the squirt and Biot mechanism: Geophysics, **58**, 524–533.

Endres, A. L., and Knight, R., 1991, The effects of pore scale fluid distribution on the physical properties of partially saturated tight sandstones: J. Appl. Phys., **69**, 1091–1098.

Eshelby, J. D., 1957, The determination of the elastic field of an ellipsoidal inclusion, and related problems: Proc. Roy. Soc. London, Ser. A, **241**, 376–396.

Gassmann, F., 1951, Uber die elastizität poröser medien: Vierteljahresschr. Naturforsch. Ges. Zurich, **96**, 1–21.

Gregory, A. R., 1976, Fluid saturation effects on dynamic elastic properties of sedimentary rocks: Geophysics, **41**, 895–921.

Hashin, Z., and Shtrikman, S., 1963, A variational approach to the theory of the elastic behavior of multiphase materials: J. Mech. Phys. Solids, **11**, 127–140.

Hill, R., 1963, Elastic properties of reinforced solids: Some theoretical principles: J. Mech. Phys. Solids, **11**, 357–372.

Jones, T. D., 1986, Pore fluids and frequency-dependent wave propagation in rocks: Geophysics, **51**, 1939–1953.

Knight, R., and Nolen-Hoeksema, R., 1990, A laboratory study of the dependence of elastic wave velocities on pore scale fluid distribution: Geophys. Res. Lett., **17**, 1529–1532.

Knight, R., and Nur, A., 1987, Geometrical effects in the dielectric response of partially saturated sandstones: Log Analysis, **28**, 513–519.

Korringa, J., Brown, R. J. S., Thompson, D. D., and Runge, R. J., 1979, Self-consistent imbedding and the ellipsoidal model for porous rocks: J. Geophys. Res., **84**, 5591–5598.

Korringa, J., and Thompson, D. D., 1977, Comment on the self-consistent imbedding approximation in the theory of elasticity of porous media: J. Geophys. Res., **85**, 933–934.

Kuster, G. T., and Toksöz, M. N., 1974, Velocity and attenuation of seismic waves in two-phase media: Part I. theoretical formulations: Geophysics, **39**, 587–606.

Mavko, G., and Jizba, D., 1991, Estimating grain-scale fluid effects on velocity dispersion in rocks: Geophysics, **56**, 1940–1949.

Milton, G. W., 1984, Correlation of the electromagnetic and elastic properties of composites and microstructure corresponding with effective medium approximations, *in* Johnson, D. L. and Sen, P. N., Eds., Physics and Chemistry of porous media: Am. Inst. Phys., 66–77.

Murphy, W. F., 1984a, Sonic and ultrasonic velocities: Theory versus experiment: Geophys. Res. Lett., **12**, 85–88.

——— 1984b, Acoustic measures of partial gas saturation in tight sandstones: J. Geophys. Res., **89**, 11549–11559.

Murphy, W. F., Winkler, K. W., and Kleinberg, R. L., 1986, Acoustic relaxation in sedimentary rocks: Dependence on grain contacts and fluid saturation: Geophysics, **51**, 757–766.

Norris, A. N., 1985, A differential scheme for the effective moduli of composites: Mech. Mater., **4**, 1–16.

——— 1989, An examination of the Mori-Tanaka effective medium approximation for multiphase composites: J. Appl. Mech., **56**, 83–88.

O'Connell, R. J., and Budiansky, B., 1977, Viscoelastic properties of fluid-saturated cracked solids: J. Geophys. Res., **82**, 5719–5736.

Thomsen, L., 1985, Biot-consistent elastic moduli of porous rocks: Low-frequency limit: Geophysics, **50**, 2797–2807.

Toksöz, M. N., Cheng, C. H., and Timur, A., 1976, Velocities of seismic waves in porous rocks: Geophysics, **41**, 621–645.

Wang, Z., Hirsche, W. K., and Sedgwick, G., 1991, Seismic velocities in carbonate rock: J. Can. Petr. Tech., **30**, 112–122.

Wang, Z., and Nur, A., 1990, Dispersion analysis of acoustic velocities in rock: J. Acoust. Soc. Am., **87**, 2384–2395.

Winkler, K. W., 1985, Dispersion analysis of velocity and attenuation in Berea sandstone: J. Geophys. Res., **90**, 6793–6800.

——— 1986, Estimates of velocity dispersion between seismic and ultrasonic frequencies: Geophysics, **51**, 183–189.

Wu, T. T., 1966, The effect of inclusion shape on the elastic moduli of a two-phase material: Int. J. Solids Structures, **2**, 1–8.

## APPENDIX A

### RESPONSE OF A COMMUNICATING SPHEROIDAL INCLUSION

Let us consider a randomly oriented spheroidal inclusion when complete fluid pressure communication occurs. To estimate the incremental strain within this inclusion, it is assumed that it is embedded in a homogeneous, infinite background having elastic moduli $k_b$ and $\mu_b$. When this system is subjected to an applied incremental strain field that has uniform cubical dilatation and deviatoric components $\partial\theta^A$ and $\partial e_{ij}^A$, respectively, at infinity, an incremental change in fluid pressure $\partial p_f$ is induced in the inclusion. The corresponding incremental applied stress at infinity is

$$\partial\sigma_{ij}^A = k_b\partial\theta^A\delta_{ij} + 2\mu_b\partial e_{ij}^A, \tag{A-1}$$

where $\delta_{ij}$ is the Kronecker delta.

Using the method of equivalent inclusions (Eshelby, 1957), it can be shown that

$$\begin{aligned}-\partial p_f\delta_{ij} = {} & k_b(\partial\theta^C + \partial\theta^A - \partial\theta^T)\delta_{ij} \\ & + 2\mu_b\big(\partial e_{ij}^C + \partial e_{ij}^A - \partial e_{ij}^T\big),\end{aligned} \tag{A-2}$$

where the superscripts $C$ and $T$ denote the "constrained" and "stress-free transformation" incremental strains, respectively, used in that analysis. The components of the uniform incremental strain within the inclusion are

$$\partial\theta^{\text{inc}} = \partial\theta^C + \partial\theta^A \tag{A-3}$$

and

$$\partial e_{ij}^{\text{inc}} = \partial e_{ij}^C + \partial e_{ij}^A. \tag{A-4}$$

Let us define the quantities $\partial\sigma_{ij}^E$, $\partial\theta^E$ and $\partial e_{ij}^E$ as follows:

$$\partial\sigma_{ij}^E = \partial\sigma_{ij}^A + \partial p_f\delta_{ij} \tag{A-5}$$

and

$$\partial\sigma_{ij}^E = k_b\partial\theta^E\delta_{ij} + 2\mu_b\partial e_{ij}^E. \tag{A-6}$$

Using these quantities, equation (A-2) can be rewritten as

$$k_b(\partial\theta^C + \partial\theta^E - \partial\theta^T)\delta_{ij} + 2\mu_b\big(\partial e_{ij}^C + \partial e_{ij}^E - \partial e_{ij}^T\big) = 0. \tag{A-7}$$

This equation describes the behavior of an identically shaped cavity when the applied incremental stress at infinity is $\partial\sigma_{ij}^E$.

The expected value of the components of the uniform incremental strain within such a randomly oriented cavity are (Berryman, 1980b)

$$\partial\theta^{\text{cav}} = P(k_b, \mu_b, 0, 0, \alpha)\partial\theta^E \tag{A-8}$$

and

$$\partial e_{ij}^{\text{cav}} = Q(k_b, \mu_b, 0, 0, \alpha)\partial e_{ij}^E. \tag{A-9}$$

The incremental strain within the cavity are related to the other strain quantities by

$$\partial\theta^{\text{cav}} = \partial\theta^C + \partial\theta^E \tag{A-10}$$

and

$$\partial e_{ij}^{\text{cav}} = \partial e_{ij}^C + \partial e_{ij}^E. \tag{A-11}$$

Hence, equations (A-8) and (A-9) can be expressed as

$$\big(\partial\theta^{\text{inc}} + \partial p_f/k_b\big) = \big(\partial\theta^A + \partial p_f/k_b\big)P(k_b, \mu_b, 0, 0, \alpha) \tag{A-12}$$

and

$$\partial e_{ij}^{\text{inc}} = Q(k_b, \mu_b, 0, 0, \alpha)\partial e_{ij}^A. \tag{A-13}$$

## APPENDIX B

### ESTABLISHING THE EQUIVALENCE BETWEEN INCLUSION-BASED APPROXIMATIONS AND GASSMANN-BIOT THEORY

The inclusion-based analogs for the open system moduli $k_{\text{open}}^*$ and $\mu_{\text{open}}^*$ are obtained by using an infinitely compressible fluid (i.e., $k_f = 0$) in the various approximations. In the case of the dilute volumetric average approximation, equations (22) and (23) give

$$k_{\text{open}}^* = k_m[1 - \phi\bar{\gamma}(k_m, \mu_m, 0, 0)] \tag{B-1}$$

and

$$\mu_{\text{open}}^* = \mu_m[1 - \phi\bar{\chi}(k_m, \mu_m, 0, 0)]. \tag{B-2}$$

Using equations (28) and (29), the Kuster-Toksöz approximation yields

$$k_{\text{open}}^* = k_m\frac{3k_m + 4\mu_m - 4\phi\mu_m\bar{\gamma}(k_m, \mu_m, 0, 0)}{3k_m + 4\mu_m + 3\phi k_m\bar{\gamma}(k_m, \mu_m, 0, 0)} \tag{B-3}$$

and

$$\mu_{\text{open}}^* = \mu_m\frac{15k_m + 20\mu_m - \phi(9k_m + 8\mu_m)\bar{\chi}(k_m, \mu_m, 0, 0)}{15k_m + 20\mu_m + 6\phi(k_m + 2\mu_m)\bar{\chi}(k_m, \mu_m, 0, 0)}. \tag{B-4}$$

The open system moduli for the EIAS approximation obtained from equations (34) and (35) are

$$k_{\text{open}}^* = k_m\{(1-\phi)/[(1-\phi) + \phi\bar{\gamma}(k_m, \mu_m, 0, 0)]\} \tag{B-5}$$

and

$$\mu_{\text{open}}^* = \mu_m\{(1-\phi)/[(1-\phi) + \phi\bar{\chi}(k_m, \mu_m, 0, 0)]\}. \tag{B-6}$$

The dilute interaction energy approximations of open system moduli given by equations (50) and (51) are

$$k^*_{\text{open}} = k_m/[1 + \phi\bar{\gamma}(k_m, \mu_m, 0, 0)] \tag{B-7}$$

and

$$\mu^*_{\text{open}} = \mu_m/[1 + \phi\bar{\chi}(k_m, \mu_m, 0, 0)]. \tag{B-8}$$

The equivalence of these inclusion-based approximations with the Gassmann-Biot theory is established by replacing $k_{\text{open}}$ and $\mu_{\text{open}}$ in equations (52) and (53) with the appropriate expressions obtained for $k^*_{\text{open}}$ and $\mu^*_{\text{open}}$ given above. In the case of the dilute volumetric average approximation, this leads to the following for the bulk moduli:

$$\begin{aligned} k_{\text{closed}} = {} & k_m\{k_f\{k_m - k_m[1 - \phi\bar{\gamma}(k_m, \mu_m, 0, 0)]\} \\ & + \phi k_m[1 - \phi\bar{\gamma}(k_m, \mu_m, 0, 0)] \\ & \times (k_m - k_f)\}/\{k_f\{k_m - k_m[1 - \phi\bar{\gamma}(k_m, \mu_m, 0, 0)]\} \\ & + \phi k_m(k_m - k_f)\}. \end{aligned} \tag{B-9}$$

This expression can be simplified to

$$k_{\text{closed}} = k_m + \frac{\phi k_m(k_f - k_m)\bar{\gamma}(k_m, \mu_m, 0, 0)}{k_m + k_f[\bar{\gamma}(k_m, \mu_m, 0, 0) - 1]}; \tag{B-10}$$

hence, it is established that $k_{\text{closed}} = k^*_{\text{com}}$ for this approximation. Following this procedure, the same result can be shown for the other three inclusion-based approximations. For the shear moduli, it can be seen that $\mu^*_{\text{open}} = \mu^*_{\text{com}}$ for all four approximations. It follows that when $\mu^*_{\text{open}}$ replaces $\mu_{\text{open}}$ in equation (53), we obtain $\mu_{\text{closed}} = \mu^*_{\text{com}}$ in all four cases. Hence, the relationships between the inclusion-based analogs for the open and closed system moduli predicted by these four inclusion-based approximations are identical to the Gassmann (1951) poroelastic relationships.